Journal of Computational and Applied Research in Mechanical Engineering

jcarme.sru.ac.ir

SRTTU

JCARME

ISSN: 2228-7922

Research paper

Vibration characteristics of rotor systems with disk-shaft clearance

Zhinong Li[a,*], Fang Qiao[a], Yunlong Li[b], Shiyao Chen[a], Shijian Zhou[a] and Fei Wang[c]

[a]Key Laboratory of Nondestructive Testing of the Ministry of Education, Nanchang Hangkong University, Nanchang, Jiangxi, 330063, China
[b]School of Mechanical Engineering, Guangxi University, Nanning, Guangxi, 530004, China
[c]School of Aircraft Engineering, Nanchang Hangkong University, Nanchang, Jiangxi 330063, China

Abstract

Currently, the existing study on rotor system with disk-shaft clearance primarily focuses on analyzing factors such as interference force and friction coefficient while neglecting the vibration characteristics during the rotational states. Therefore, a finite element model is established by taking rotor systems with disk-shaft clearance as the research object. The vibration characteristics of rotor systems under different clearances or rotation speeds are analyzed. Increasing clearance leads to gradual fluctuations in the speed difference of shaft to disk, accompanied by an increasing periodicity of these fluctuations. In the time domain diagram, beat vibration characteristic become evident, and its period undergoes noticeable changes. The amplitude of rotation frequency increases, while that of multiple frequency decreases gradually and tends to a constant value. The presence of clearance causes the orbit of the disk center to become an irregular circle, and the shape of 8 appears. Additionally, collision and friction of shaft to disk result in apparent serrations in the orbit. As the rotational speed increases, the speed difference initially increases but eventually reaches a stable value. The beat vibration characteristic disappears due to the small speed difference, leading to a small amplitude of the multiple frequency. The orbit of the disk center tends to become circular, and the serrated phenomenon weakens and disappears. Finally, the experiments of rotor systems with disk-shaft clearance are carried out. The results are in good agreement with the simulations, which verifies the correctness of the dynamic model. The research results can provide a theoretical basis for understanding rotor systems with disk-shaft clearance.

1. Introduction

Loosening in rotating machinery often occurs due to poor assembly quality or long-term exposure to vibration and shock [1, 2]. The loosening of rotor systems has been studied. Baek *et al.* [3] conducted numerical analysis on

the vibration loosening of screw fasteners, proposing a calculation formula for the loosening process and verifying it by looseness test. Their experimental results were in good agreement with the theoretical predictions. The reduction of clamping force in bolted connection under cyclic separation load was analyzed by

experimental and numerical methods [4]. The results revealed that thread loosening increases with eccentricity and decreases with the initial clamping force. A finite element model was established based on the evolution of wear on the thread surface [5]. The results demonstrated that fretting wear resulting from changes in the distribution and size of contact stress between threads led to a reduction in clamping force and an increase in the radial sliding distance of the thread. A dynamic model was established for the double-rotor systems with bearing seat loosening, and the dynamic characteristics of both the internal and external rotors were investigated [6]. The research focused on a bolt connecting a disk and a shaft [7]. The influencing factors of bolt looseness were analyzed, and their impact on rotor dynamics was further studied. A rotor system with foundation loosening was modeled by simulation, and the influence of parameters on the dynamic characteristics of rotor systems was analyzed [8]. It should be noted that the literature primarily studied the dynamic characteristics of non-rotating parts [9]. However, considering that the disk and shaft are the main power components of rotor systems, their contact area is prone to clearance because of rotation speed, temperature, and wear.

The main factors influencing shaft-hub motion have been analyzed. Liao *et al.* [10] conducted an example using a turbocharger compressor, examining the impact of rotation speed, interference amount, and friction factor on the contact stress of the shaft-hub. The results revealed that increasing rotational speed led to the separation of contact points in regions with high radial values of the impeller, accompanied by the sliding phenomenon within the middle-contact area between the impeller and the shaft sleeve. Investigating the gear hub and shaft matching failure, Truman *et al.* [11] elucidated the cause of motion and slip, employing finite element methods to simulate faulty systems with results aligning closely with the experiment. Xiang *et al.* [12] delved into the factors influencing the fatigue of wheel-shaft motion in high-speed trains. It is found that global slip happens in the contact area when there is a large relative displacement between the wheel and

shaft, severely diminishing fatigue life. Duan *et al.* [13] explored in-flight parking caused by tenon fracture in a four-stage engine compressor, attributing the fracture to fretting wear fatigue due to improper contact between tenon and mortise. The radial fretting in the compressor's shaft-hub was studied, and the influence of interference fit and rotational speed was analyzed [14]. Lu [15] established a finite element model for shaft-hub under two assembly modes, evaluating the influence of interference fit, friction coefficient, rotating speed, and preloading forces on radial fretting characteristics. Finite element method was used to analyze the stress variation and distribution on the material contact surface subjected to fretting load [16]. Peng *et al.* [17] examined the influence of contact pressure on the fretting damage of aluminum alloy materials, revealing a significant increase in damage with elevated contact pressure. Overall, these studies shed light on the influence factors governing fretting and slippage at the interface of shaft-hub contact. The shaft-hub friction caused by clearance can lead to system malfunctioning. Considering that shaft-hub clearance occurs during rotor rotation, investigating the dynamic characteristics of rotor systems with shaft-hub loosening is crucial for early fault detection purposes.

Behzad and Asayesh [18, 19] investigated the vibration characteristics of shaft-hub loosening. He established a contact model for disk-shaft large clearance based on the assumption that the disk was always in contact with the shaft. He also studied the nonlinear dynamic behavior of rotors at different speeds. Subsequent research by Wei *et al.* [20, 21] and Li *et al.* [22-25] focused on improving the contact model. In these papers, the shaft-hub clearance was equated to the disk's eccentricity. However, employing the equivalent makes it challenging to discern the motion of friction and sliding accurately.

The present research is focused on the rotor system featuring a disk-shaft clearance and establishes the finite element model of the system. Then, the vibration characteristics of the rotor system are studied. How the vibration characteristics evolve is mainly explored. The validity of the finite element model is verified by experiments. These obtained outcomes provide

theoretical support for the fault diagnosis of the disc-shaft system with a slight loose disc in engineering practice.

2. Vibration model of rotor systems with disk-shaft clearance

Due to the fitting failure, disk-shaft clearance is commonly observed in rotor systems. Fig. 1(a) shows the rotor system model [26], and Fig. 1(b) shows the cross-section diagram of disk-shaft contact [27, 28]. Specifically, O_1 and O_2 are the centers of shaft and disk, respectively. When a clearance occurs, rubbing occurs simultaneously, resulting in thermal deformation and variations in local mass, stiffness, damping, and friction coefficient within the rotor systems. As a consequence, the resulting nonlinear factors become complex. To simplify the study [29], thermal changes were omitted, and only the variation characteristics of force and motion were analyzed.

During the rubbing process, the force at the contact point can be decomposed into tangential and radial directions. Tangential force F_τ and radial force F_n can be expressed as:

$$\begin{cases} F_n = k \cdot x \\ F_\tau = \mu \cdot k \cdot x \end{cases} \tag{1}$$

where μ is the coefficient of disk-shaft friction and k is the contact stiffness.

According to the translation relationship in rigid body mechanics, F_τ is equivalent to a torque M and a radial force F across the shaft, that is:

$$F = \sqrt{F_n{}^2 + F_\tau{}^2} = \sqrt{1+\mu^2} \cdot k \cdot x \tag{2}$$

$$M = R \cdot F_\tau = R \cdot \mu \cdot k \cdot x \tag{3}$$

where R is the radius of shaft. Assuming that the relative velocity of shaft to disk at the contact point is v, it can be obtained:

$$F = \sqrt{1+\mu^2} \cdot k \cdot x = \sqrt{1+\mu^2} \cdot k \cdot v \cdot t \tag{4}$$

$$M = R \cdot \mu \cdot k \cdot x = R \cdot \mu \cdot k \cdot v \cdot t \tag{5}$$

where t is the time. In regular circumstances, the disk-shaft friction occurs intermittently. The separation and contact of disk-shaft appear alternately. When the friction degree is relatively high, the shaft always contacts the disk, and the slip does not occur. As the contact depth increases, the force at the contact point also increases. For the research convenience, the contact variations in this process are regarded as linear changes. Eq. (6) is the motion equation of the nodes in the rotor structure [30, 31].

$$[M]\{u''\} + [C + C']\{u'\} + [K + K_1]\{u\} = \{F(t)\} \tag{6}$$

where M, C, C', K, and K_1 are the matrixs of mass, damping, contact damping, stiffness, and contact stiffness of rotor systems, respectively [32, 33]. u'', u' and u are the acceleration, velocity, and displacement of structure nodes, respectively.

If damping is ignored, Eq. (6) can be written as:

$$[M]\{u''\} + [K + K_1]\{u\} = \{F(t)\} \tag{7}$$
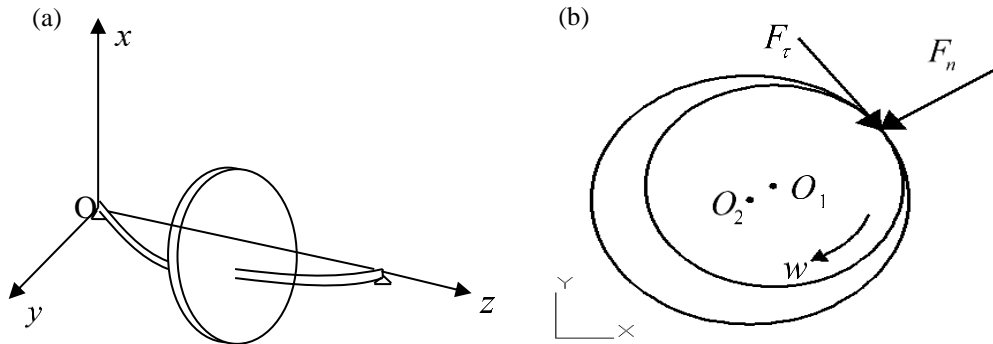
Fig. 1. Model of rotor system with clearance disk-shaft; (a) rotor model of Jeffcott and (b) cross-section diagram of disk-shaft contact.

Because the rotor moves with respect to the fixed coordinate system A_{xy}, the displacement of the rotor nodes in the x and y directions is u_x and u_y.

$$\begin{cases} u_x = A_x \cos(w_n t + \varphi_x) \\ u_y = A_y \cos(w_n t + \varphi_y) \end{cases} \tag{8}$$

The Newmark time integral method is used to solve the Eq. (7).

$$u'_{t+\Delta t} = u'_t \Delta t + \left[(1-\delta)u''_t + \alpha u''_{t+\Delta t}\right]\Delta t \tag{9}$$

$$u_{t+\Delta t} = u_t + u'_t \Delta t + \left[(\frac{1}{2}-\alpha)u''_t + \alpha u''_{t+\Delta t}\right]\Delta t^2 \tag{10}$$

where δ and α are constants related to the accuracy and stability of the calculation process. Firstly, the initial calculation is carried out to determine M, K, and C. Meanwhile, u, u', and u'' are given, and Δt, δ and α are determined. $\hat{K}$ is the effective stiffness matrix.

$$\hat{K} = K + c_0 M + c_1 C \tag{11}$$

Eq. (12) is the decomposition of $\hat{K}$.

$$\hat{K} = LDL^T \tag{12}$$

Then, the effective payload $\hat{Q}_{t+\Delta t}$, displacement $u_{t+\Delta t}$, velocity $u'_{t+\Delta t}$ and acceleration $u''_{t+\Delta t}$ at time $t+\Delta t$ can be obtained.

$$LDL^T u_{t+\Delta t} = \hat{Q}_{t+\Delta t} \tag{13}$$

$$u'_{t+\Delta t} = u'_t + c_6 u''_t + c_7 u''_{t+\Delta t} \tag{14}$$

$$u''_{t+\Delta t} = c_0(u_{t+\Delta t} - u_t) - c_2 u'_t - c_3 u''_t \tag{15}$$

The clearances can affect the dynamic characteristics of rotor systems. Based on finite element theory, the contact model of disk-shaft clearance is studied. The geometric model of the disk-shaft is established in Solidworks. Ansys is used to mesh the geometric model, impose constraints, and loads.
The materials of disk and shaft are set as #45 steel, whose parameters are shown in Table 1. The simplified model of rotor systems is shown in Fig. 2.
Solid1086 element is used to establish the model

[34]. There is friction contact between the shaft and the disk. The clearance can be controlled by adjusting the offset. Spring-simulated bearings are applied to both ends of the shaft.
The shaft and disk are meshed by hexahedron automatically. To simplify the calculation, the shaft's lateral displacement is constrained, and all the translational and rotational degrees of freedom of the disk are released. Meanwhile, gravity is applied to the system, and the load is added in the form of shaft velocity.

3. Simulation research

The finite element modeling and simulation of rotor systems with disk-shaft clearance are carried out. The characteristics of time-frequency, the orbit of the disk center, and the speed difference of the disk-shaft are analyzed under different clearances and speeds.

3.1. Analysis of time-frequency

Fig. 3 shows the time-frequency diagram of the rotor system with different clearances when the shaft velocity is 1800 rpm. When the clearance is 0 mm, only the normal rotation frequency of 30 Hz appears. The obvious beat vibration characteristic appears with the increasing clearance.

Table 1. Performance parameters of materials.

Description	Value
Length of shaft (L_s)	422 mm
Radius of shaft (R)	4.75 mm
Thick of disk (t_d)	12.5 mm
Inner radius of disk (R_{id})	4.75 mm
Outer radius of disk (R_{od})	38.1 mm
Density (ρ)	7890 kg/m^3
Modulus of elasticity (E)	209 GPa
Poisson's ratio (ν)	0.269
Spring stiffness (k_x, k_y)	1.3×10^7 N/m
Spring damping (c_x, c_y)	7×10^2 Ns/m
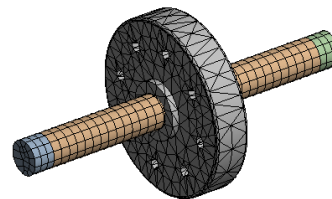
Fig. 2. Simplified model of rotor systems.
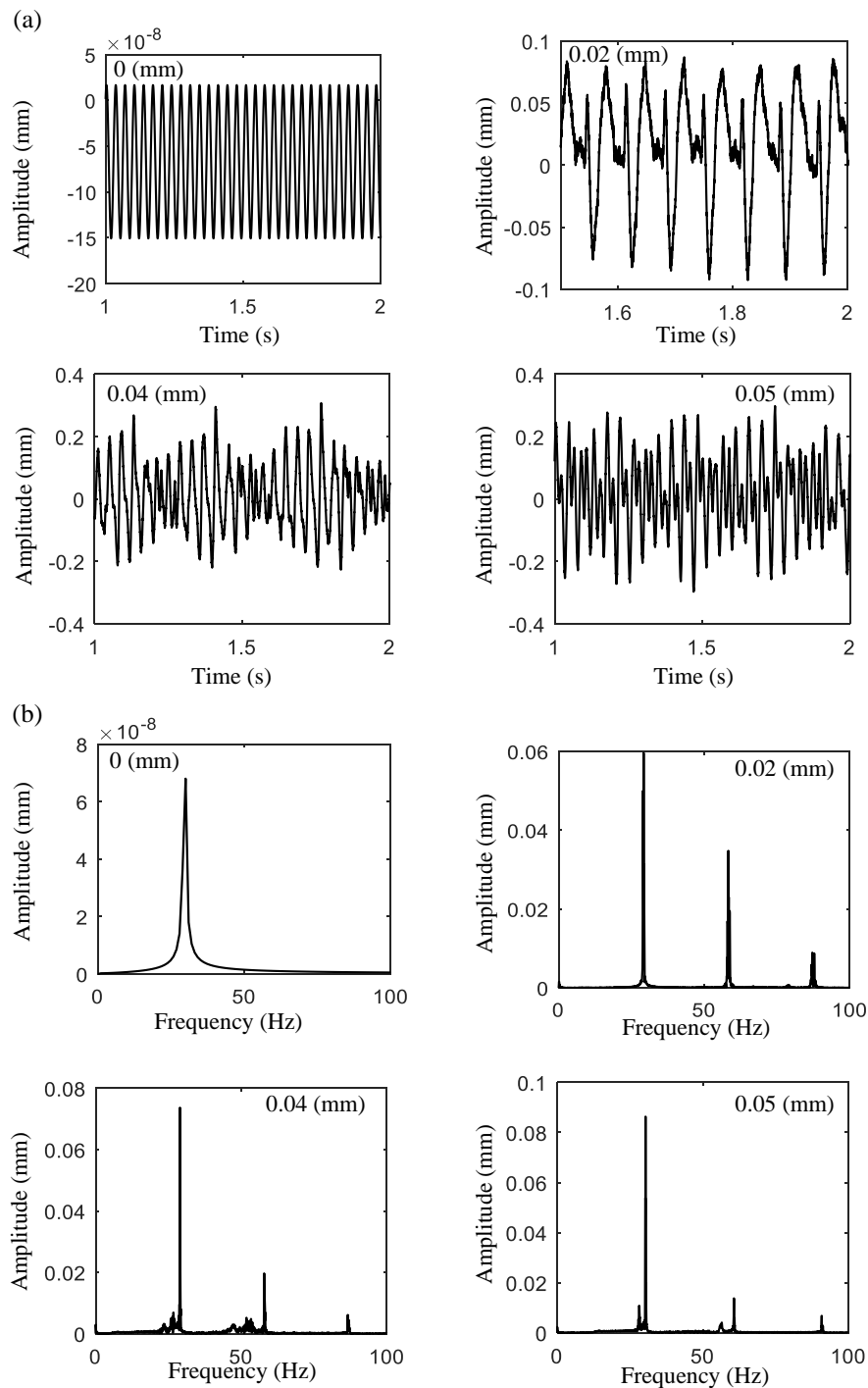
Fig. 3. Time-frequency diagram of the system with different clearances at 1800 rpm; (a) time-domain diagram and (b) frequency-domain diagram.

The beat vibration is caused by disk-shaft slip due to the clearance. While the period of the beat vibration changes with the clearance. The normal rotation frequency of 30 Hz and obvious multiple frequencies occur in the spectrum diagram when the clearance is 0 mm. One frequency with a very small difference occurs when the clearance is 0.02 mm, namely, the rotation frequency of the shaft is 30 Hz, and that of the disk is 29.95 Hz.

Because the two frequencies coincide, the beat characteristic occurs. The multiple frequency is mainly caused by the collision of the shaft to the disk. When the clearance is 0.04 mm, there are also obvious multiple frequencies and a frequency of 29.8 Hz. The amplitudes of multiple frequencies significantly are reduced. However, the amplitude of the rotating frequency increases with the clearance. There are also obvious multiple frequencies and a frequency of 29.7 Hz when the clearance is 0.05 mm. Through comparison and analysis of Fig. 3, it can be found that the sliding phenomenon of the disk-shaft occurs when there is a clearance. At this point, the rotation frequency of the disk is close to that of the shaft. After the superposition of the two frequencies, a beat vibration characteristic appears, and its period changes with the clearance. Due to the collision of shaft-disk, there are obvious multi-frequency components in the spectrum. The amplitude of rotating frequency increases with the clearance. The time-frequency diagram in Fig. 4(a) and Fig. 4(b) represent the vibration characteristics of the rotor system with a clearance of 0.02 mm at different shaft speeds. In Fig. 4(a), obvious beat vibration characteristic appears. The rotation frequency of the shaft is 35 Hz, and that of the disk is 34.91 Hz. The amplitudes of multiple frequencies are small relative to the rotating

frequency. In Fig. 4(b), there are no beat vibration characteristics. The rotation frequency of the shaft is 39.9 Hz, and that of the disk is 39.85 Hz. Meanwhile, the amplitude of multiple frequencies is very small.

By comparing and analyzing Fig. 3 with Fig. 4, the beat vibration period changes with the shaft velocity when the clearance is 0.02 mm. The beat vibration phenomenon gradually disappears. The amplitude of multiple frequencies decreases sharply until it cannot be seen. Therefore, when there is a clearance, the collision vibration of the disk-shaft decreases greatly with the shaft speed.

3.2. Analysis of disk center orbit

Fig. 5 shows disk center orbits of rotor system at different clearances when the shaft speed is 1800 rpm. The orbit is a regular circle when the clearance is 0 mm. When the clearance is 0.02 mm, the orbit is a shape of 8. At the same time, irregular sawtooth phenomenon appears. The orbit with obvious serrated phenomenon becomes more irregular when the clearance is 0.04 mm and 0.05 mm. The sawtooth phenomenon is mainly caused by the disk-shaft collision during rotation. Analysis of Fig. 5 shows that the movement of the disk changes from regular to irregular collision when the contact clearance of disk-shaft increases within a certain range.
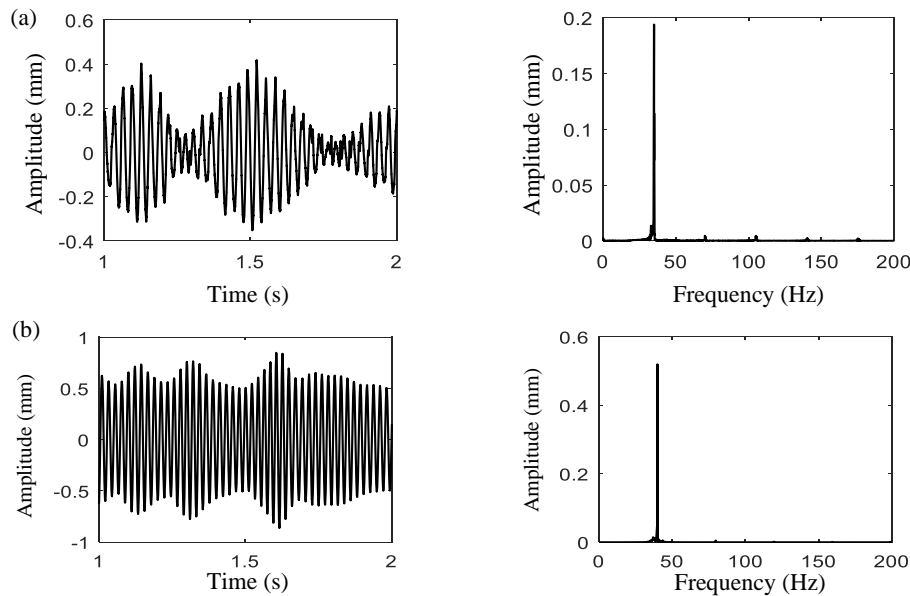

Fig. 4. Time-frequency diagram of the system with a clearance of 0.02 mm at different shaft speeds; (a) 2100 rpm and (b) 2400 rpm.
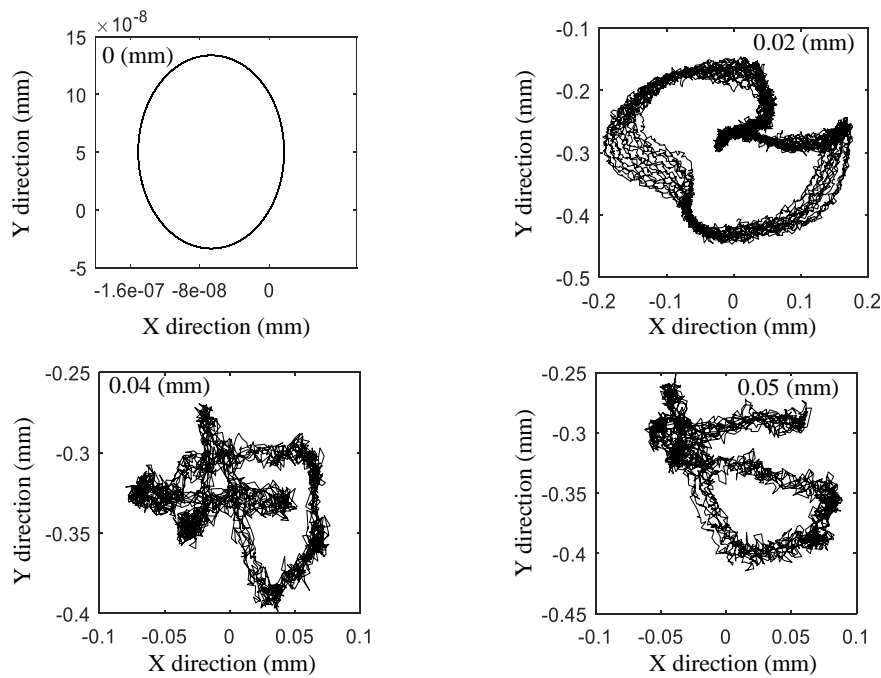
Fig. 5. Orbit of disk center at different clearances.

Fig. 6 shows the disk center orbits of the rotor system at different shaft speeds when the clearance is 0.02 mm. In Fig. 6(a), the orbit is an irregular circle with a small sawtooth phenomenon. In Fig. 6(b), the orbit is a regular circle without a sawtooth.

Comparing Fig. 5 to Fig. 6, it is not difficult to find that the orbit of the disk center is deformed into a regular circle from a shape of 8 when the shaft speed increases from 1800 rpm to 2400 rpm. And the sawtooth shape disappears, meaning that the disk-shaft collision decreases. This result is the same as the analysis results in the time-frequency domain.

3.3. Speed difference of shaft to disk

In the simulation, the velocity increased from 0 rpm to 1800 rpm at 0-1s. Then, the speed is maintained at 1800 rpm at 1 to 2 s. Therefore, the speed difference between 1 s and 2 s is analyzed. Fig. 7 shows the speed difference diagram of the shaft to disk under different clearances. The difference remains unchanged at 0.03 mm/s when the clearance is 0 mm. As the increase of the clearance, the speed difference fluctuates periodically around 0.8, 1, and 1.2 mm/s.

Fig. 8 shows the speed difference of the disk-shaft under different shaft speeds when the clearance is 0.02 mm. The speed difference fluctuates periodically around 1 mm/s when the shaft speed is 2100 rpm. And the speed difference fluctuates around 1.1 mm/s. By comparing Fig. 7 to Fig. 8, it is not difficult to find that the fluctuation of speed difference increases first and then decreases with the increase of shaft speed.

4. Experimental research

To verify the simulation results, a test system with disk-shaft clearance is designed. Fig. 9 shows the rotor test bench, which contains a motor, a coupling, a disk-shaft, and bearing supports. Flexible coupling is used to ensure that the motor only transfers torque to the shaft and reduces the vibration signal from the motor. The motor can realize step-less speed regulation of 0-10000 rpm. The diameter of the shaft is 9.5 mm, the outer diameter of the disk is 76.2 mm, the distance between the supports at both ends of the shaft is 422 mm, and the mass of the disk is 0.612 Kg. Self-lubricating graphite bearings are used in experiments.
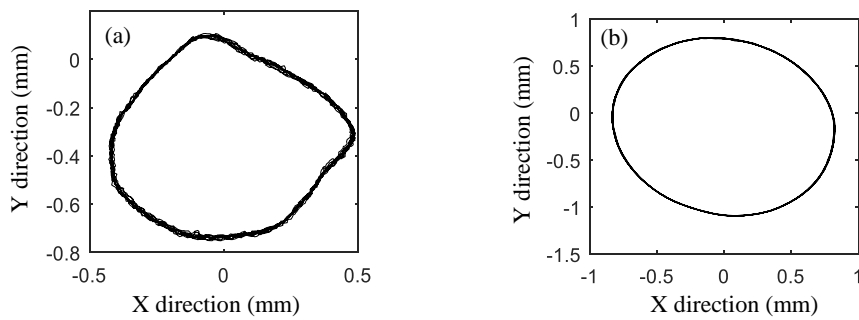
Fig. 6. Orbit of disk center at different shaft speeds; (a) 35 rad/s and (b) 40 rad/s.
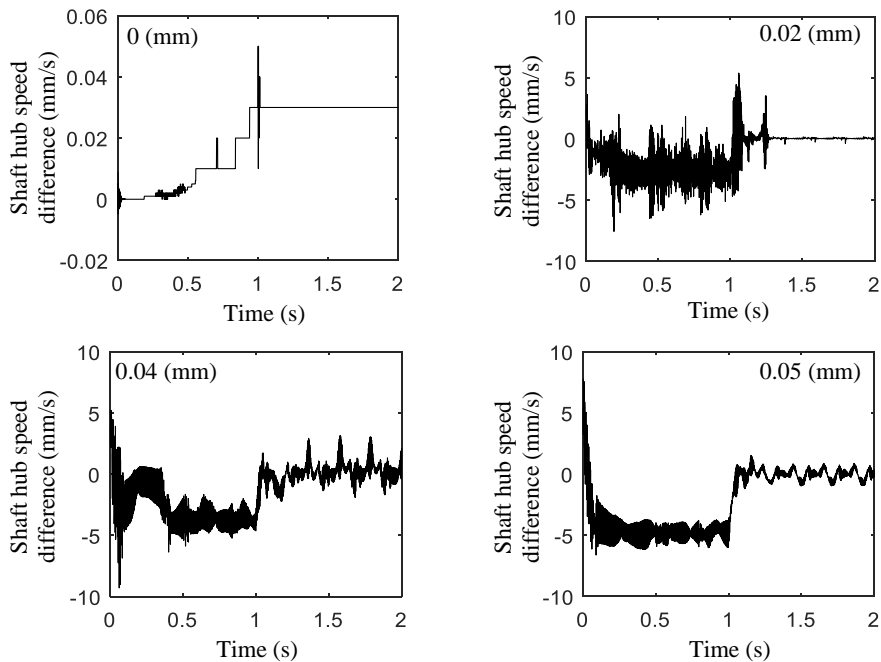
Fig. 7. Different clearance, shaft hub speed difference diagram.
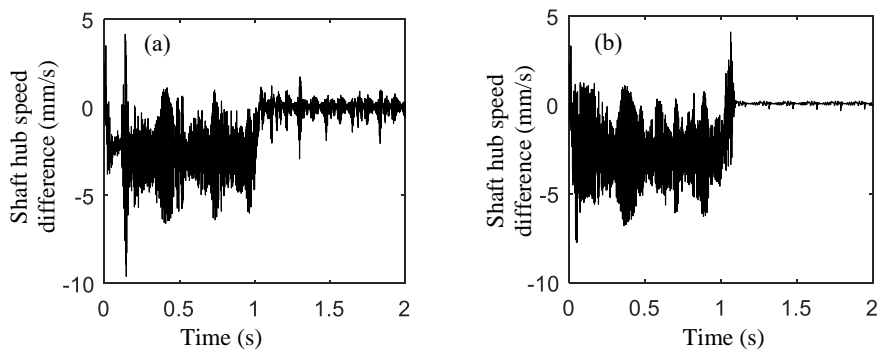
Fig. 8. Different shaft speeds, shaft hub speed difference diagram; (a) 35 rad/s and (b) 40 rad/s.

To analyze the vibration characteristics of the system with disk-shaft clearance, experiments are carried out by adjusting the clearance. The disk in the experiment consists of an inner ring and an outer ring. The two parts are connected by a thread with a conical surface. The interference force and disk-shaft clearance are adjusted by the thread.
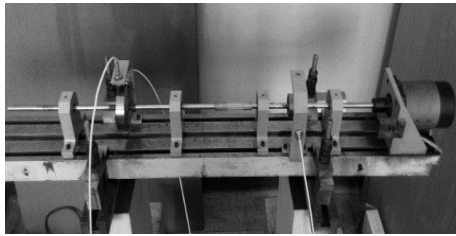
Fig. 9. ZT-3 rotor test bench.

Because the clearance is very small, the influence of lateral displacement of the disk is not considered. The displacement signals of the system were collected using an eddy current displacement transducer and DH5910A data acquisition system.

4.1. Analysis of time-frequency

Fig. 10 shows the time-frequency diagram of the system when the disk-shaft interference fits at 1620 rpm.
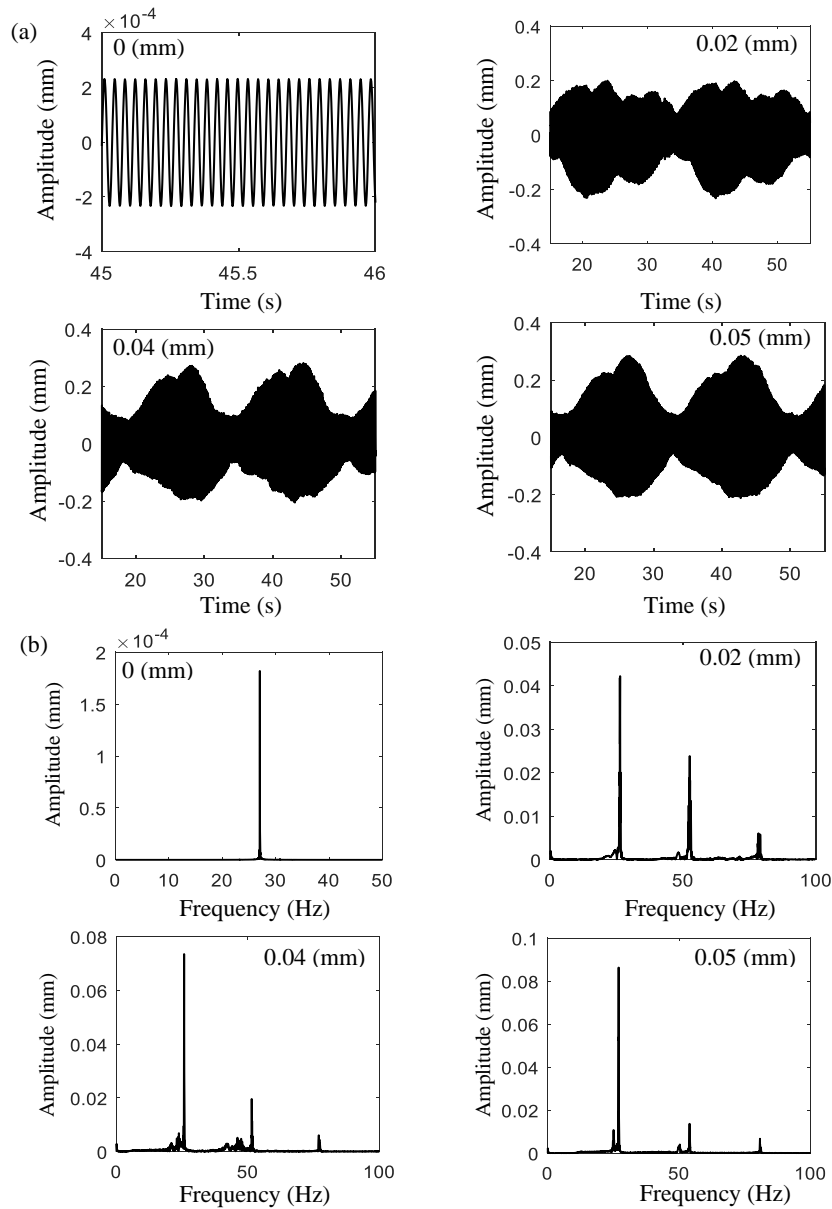

Fig. 10. Time-frequency diagram of the system with different clearances at 27 r/s; (a) time-domain diagram and (b) frequency-domain diagram.

Obvious beat vibration characteristic appears when the clearance is 0.02 mm. There is obvious beat vibration characteristic in the time-domain diagram when the clearance is 0.04 mm and 0.05 mm. While the beat vibration period changes. Only the rotation frequency of 27 Hz is in the spectrum when the clearance is 0 mm. When the clearance is 0.02 mm, there are frequencies of 27 Hz and 26.9 Hz. At the same time, there is an obvious multiple frequency. Multiple frequencies mainly comes from the disk-shaft collision vibration, which is the same as the simulation results. When the clearance is 0.04 mm, the frequencies are 26.5 Hz and 25.75 Hz, respectively. There are also obvious multiple frequencies. The maximum amplitude frequency is 26.5 Hz. When the clearance is 0.05 mm, the frequencies are 27 Hz and 25.6 Hz. There are also obvious multiple frequencies. At this time, the maximum amplitude frequency is 27 Hz.

Comparing the diagrams in Fig. 10, the beat vibration characteristic appears in the time-domain diagram of rotor systems when there is a clearance. As the clearance increases, the beat vibration period changes. Due to the disk-shaft collision, there are obvious multi-frequency components in the spectrum. The amplitude of the rotation frequency increases significantly with the clearance. However, the amplitude of multi-frequencies decreases slightly. The change characteristics of this result are the same as those of the simulation results.

Fig. 11 shows the time-frequency diagram of the rotor system under different shaft speeds when the clearance is 0.02 mm. From Fig. 11(a), there are beat vibration characteristics in the time-domain diagram. The rotation frequency of the shaft is 35 Hz, and the rotation frequency of the disk is 34.8 Hz. The amplitudes of multiple frequencies are small relative to those of the rotation frequencies. As can be seen from Fig. 11(b), no beat vibration characteristics appear in the time-domain diagram. Rotation frequencies of 42.75 Hz and 42.5 Hz are shown in the spectrum diagram. The amplitude of multiple frequencies is small.

By comparing and analyzing Fig. 10 with Fig. 11, the beating vibration phenomenon disappears with the increase in shaft speed. The amplitude of multiple frequencies in the spectrum diagram is almost invisible and decreases sharply with the shaft speed.
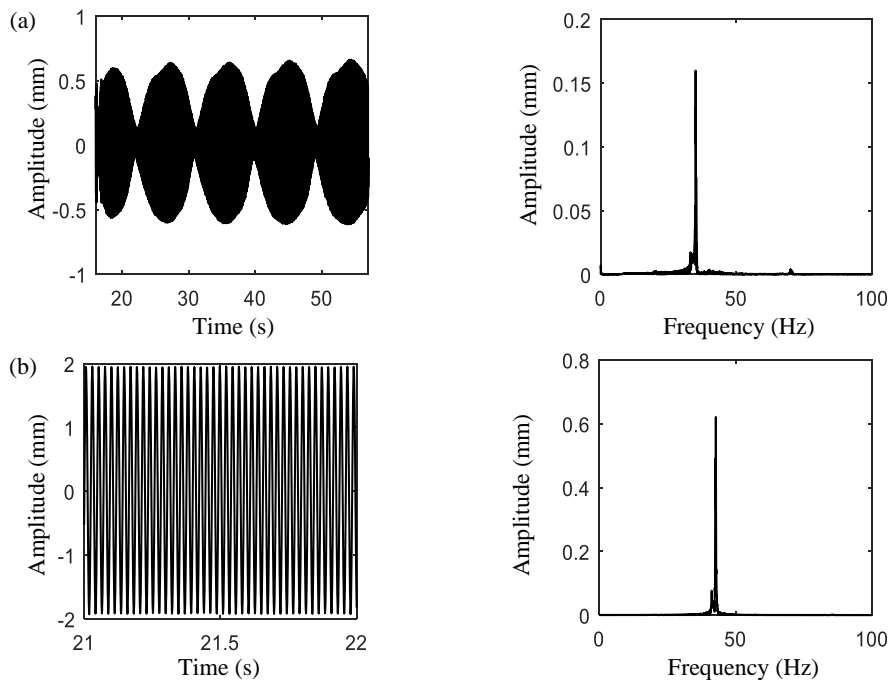

Fig. 11. Time-frequency diagram of the system with a clearance of 0.02 mm at different shaft speeds; (a) 35 r/s and (b) 43 r/s.

4.2. Analysis of disk center orbit

Fig. 12 shows the orbit of the disk center at different disk-shaft clearances at 1620 rpm. When the clearance is 0 mm, the orbit is a regular circle. It was found that the orbit changed from a regular circle to an irregular triangle as the clearance increases. Because of the collision, the orbit has obvious serrated characteristics.

Fig. 13 shows the orbit of the disk center at different speeds when the clearance is 0.02 mm. The orbit in Fig. 13(a) is an irregular circular

when the shaft velocity of 2100 rpm. There are obvious serrated characteristics in the orbit. In Fig. 13(b), the orbit shows a regular circle, and the serrated phenomenon in the orbit has disappeared.

Comparing Fig. 12 to Fig. 13, when the shaft velocity increases from 1800 rpm to 2400 rpm, the orbit changes from an irregular circular with serrated to a regular circle. The results mean that the disk-shaft collision decreases, which agrees well with the simulation results.
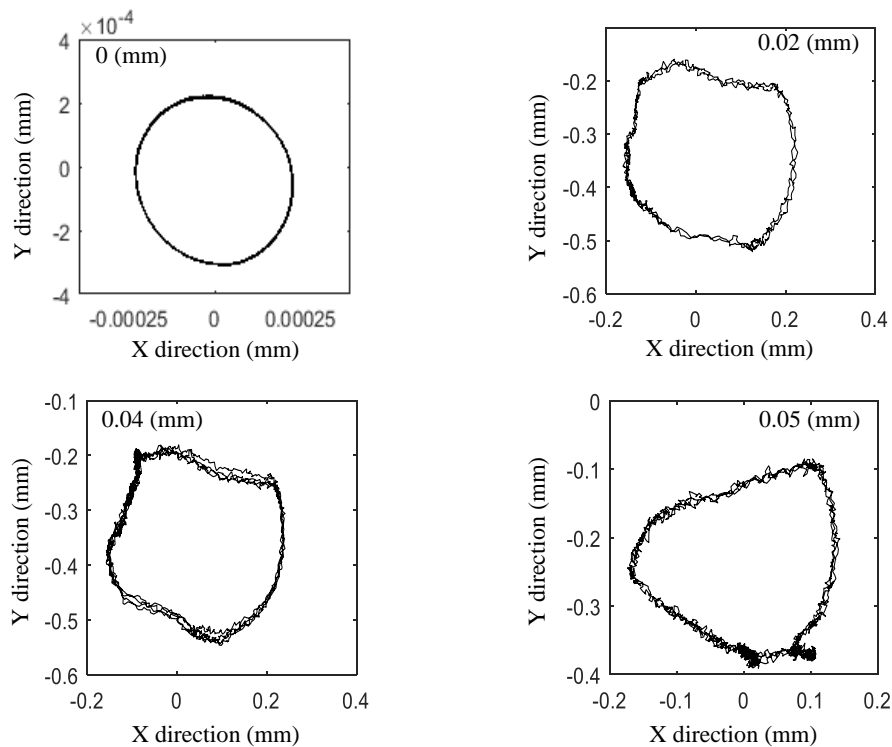

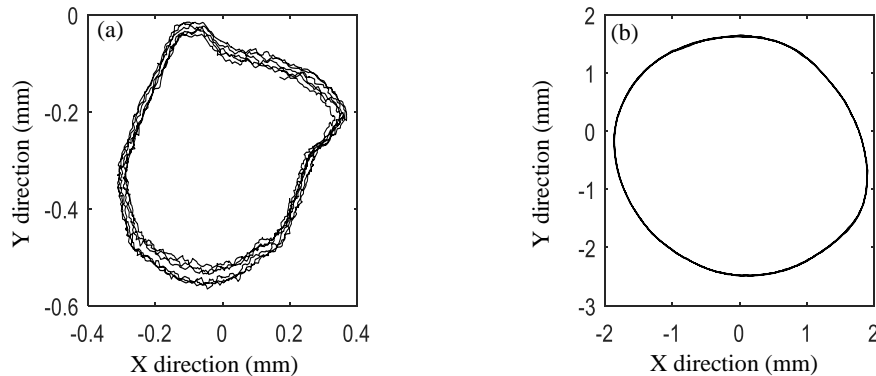**Fig. 12.** Orbit of disk center at different clearance.

Fig. 13. Orbit of disk center at different shaft speeds; (a) 35 rad/s and (b) 40 rad/s.

5. Conclusions

A finite element model of a rotor system with disk-shaft clearance is established. The vibration characteristics of the system are analyzed at different clearances and rotation speeds. By finite element simulation, the variations of the speed difference of disk-shaft, time-frequency characteristics, and orbits of disk center are discussed. Furthermore, the rationality of the finite element model is verified by experiments. The following conclusions can be drawn.

(a) When the clearance is small, the speed difference is a stable positive value, and it is not periodic fluctuant. Due to the close speed differences, there is an obvious beat vibration characteristic in the time-domain diagram. The multiple frequency components in the spectrum are clear.

(b) As the clearance increases, the speed difference fluctuates around a value, and the fluctuation periodicity becomes stronger. The beat vibration characteristic still exists in the time-domain, while the period of beat vibration changes. The amplitude of rotation frequency in the spectrum increases with the clearance, while the amplitude of multiple frequency decreases and finally tends to a constant. The orbit becomes an irregular shape of 8 with an obvious serrated characteristic due to the disk-shaft collision.

(c) With the increase of the shaft speed, the speed difference remains periodic fluctuation around a value. The amplitude of the fluctuation increases first and then decreases. The beat vibration characteristic gradually disappears. The amplitude of the rotation frequency does not change significantly, and the amplitude of the multiple frequencies decreases to a very small value. The orbit tends to be a regular circle. The serrated characteristic resulting from the disk-shaft collision disappears.

References

[1] Q. S. Cao, Q. Xiang and G. L. Xiong, "Review of Mechanical Looseness Phenomena and Failure Characteristics Study", *Noise and Vibration Control*, Vol. 35, No. 2, pp. 1-6+23, (2015).

[2] Z. N. Li, F. Qiao, W. X. Lu, J. Liu, D. Wang and F. L. Chu, "Vibration characteristics of rotor system with loose disc caused by the insufficient interference force", *Chin. J. Mech. Eng.*, Vol. 35, No. 1, pp. 70, (2022).

[3] K. H. Baek, N. T. Jeong, H. R. Hong, S. B. Choi, E. S. Lee, H. M. Kim, J. W. Kwon, S. Y. Song, H. S. Jang, H. Y. Lee and M. W. Suh, "Loosening mechanism of threaded fastener for complex structures", *J. Mech. Sci. Technol.*, Vol. 33, No. 4, pp. 1689-1702, (2019).

[4] J. H. Liu, H. J. Ouyang, Z. Q. Feng, Z. B. Cai, J. F. Peng, Y. Q. Du and M. H. Zhu, "Self-loosening of bolted L-stub connections under a cyclic separating load", *Wear*, Vol. 426-427 Part A, pp. 662-675, (2019).

[5] R. Zhang, *Study on dynamic characteristics of rotor system with foundation looseness*, MA thesis, Lanzhou Jiaotong University, Lanzhou, Gansu, (2018).

[6] H. Z. Xu, N. F. Wang and D. X. Jiang "Bearing pedestal looseness dynamic model of dual rotor system and fault feature", *J. Aerosp. Power*, Vol. 31, No. 11, pp. 2781-2794, (2016).

[7] Z. Y. Qin, Q. K. Han and F. L. Chu, "Bolt loosening at rotating joint interface and its influence on rotor dynamics", *Eng. Fail. Anal.*, Vol. 59, pp. 456-466, (2016).

[8] M. Y. Zhang, D. F. Zeng, L. T. Lu, Y. B. Zhang, Wang and J. M. Xu, "Finite

element modelling and experimental validation of bolt loosening due to thread wear under transverse cyclic loading", *Eng. Fail. Anal.*, Vol. 104, pp. 341-353, (2019).

[9] F. L. Chu and Y. Tang, "Stability and non-linear responses of a rotor-bearing system with pedestal looseness", *J. Sound Vib.*, Vol. 241, No. 5, pp. 879-893, (2001).

[10] A. H. Liao, H. W. Zhang and C. H. Wu, "FEA on frictional contact problems of impeller-shaft sleeve-shaft", *China Mechanical Engineering*, Vol. 17, No. 10, pp. 1010-1014, (2006).

[11] C. E. Truman and J. D. Booker, "Analysis of a shrink-fit failure on a gear hub/shaft assembly", *Eng. Fail. Anal.*, Vol. 14, No. 4, pp. 557-572, (2006).

[12] X. Y. Xiang, G. Q. He, B. Liu, Z. F. Hu and M. H. Zhu, "Overview of factors influencing fretting fatigue of wheel axle of high-speed train", *Materials Review*, Vol. 23, No. 1, pp. 63-66, (2009).

[13] J. K. Duan, X. Y. Yang, L. W. Dong and B, Wang, "Research on fracture of compressor blade dovetail from fretting wear", *Gas Turbine Exp. Res.*, Vol. 22, No. 3, pp. 28-32, (2009).

[14] X. Z. Huang, *Contact numerical analysis and fretting character research on shaft-hub of compressor impeller*, MA thesis, North University of China, Taiyuan, Shanxi, (2012).

[15] X. L. Lu, *Investigations on composite fretting of the shaft-hub of compressor impeller*, MA thesis, North University of China, Taiyuan, Shanxi, (2015).

[16] X. Liu, J. X. Liu, Z. X. Zuo and H. Y. Zhang, "Numerical study on residual stress redistribution of shot-peened aluminum 7075-T6 under fretting loading", *Int. J. Mech. Sci.*, Vol. 160, pp. 156-164, (2019).

[17] J. F. Peng, B. T. Wang, X. Jin, Z. B. Xu, J. H. Liu, Z. B. Cai, Z. P. Luo and M. H. Zhu, "Effect of contact pressure on torsional fretting fatigue damage evolution of a 7075 aluminum alloy", *Tribol. Int.*, Vol. 137, pp. 1-10, (2019).

[18] M. Behzad and M. Asayesh, "Vibration analysis of rotating shaft with loose disk", *IJE Transactions B: Applications*, Vol. 15, No. 4, 385-393, (2002).

[19] M. Behzad and M. Asayesh, "Numerical and experimental investigation of the vibration

of rotors with loose discs", *Proc. Inst. Mech. Eng., Part C: J. Mech. Eng. Sci.*, Vol. 224, No. 1, pp. 85-94, (2010).

[20] S. H. Wei and W. X. Lu, "Analysis on vibration characteristics of disk-shaft system with loose fit", *J. Dyn. Control*, Vol. 16, No. 3, pp. 244-249, (2018).

[21] S. H. Wei, W. X. Lu and F. L. Chu, "Speed characteristics of disk-shaft system with rotating part looseness", *J. Sound Vib.*, Vol. 469, pp. 115127, (2020).

[22] J. Liu, *Study on vibration characteristics of rotors with loose disc*, MA thesis, Nanchang Hangkong university, Nanchang, Jiangxi, (2018).

[23] J. Liu, Z. N. Li and W. X. Lu, "Effects of unsteady oil film force on rotor system with loose disk and shaft", *J. Vib. Shock*, Vol. 38, No. 17, pp. 268-275, (2019).

[24] Z. N. Li, J. Liu, W. X. Lu and F. L. Chu, "Research on dynamic modeling and simulation of rotors with loose disc", *J. Mech. Eng.*, Vol. 56, No. 7, pp. 60-71, (2020).

[25] S. J. Zhou, S. Y. Chen, Z. N. Li, C. Z. Chen and W. X. Lu, "Characteristics of rotor system with shaft-hub micro-motion subjected to interference failure", *J. Shenyang Univ. Technol.*, Vol. 43, No. 4, pp. 413-419, (2021).

[26] Z. N. Li, Y. L. Li, D. Wang, Z. K. Peng and H. F. Wang, "Dynamic Characteristics of rotor system with a slant crack based on fractional damping", *Chin. J. Mech. Eng.*, Vol. 34, No. 1, p. 27, (2021).

[27] R. R. Mutra and J. Srinivas, "An optimization-based identification study of cylindrical floating ring journal bearing system in automotive turbochargers", *Meccanica*, Vol. 57, No. 5, pp. 1193–1211, (2022).

[28] X. X. Qu, G. Chen and B, Qiao, "Signal separation technology for dynamic model of rotor with unbalance-rubbing-looseness couped faults". *J. Vib. Shock*, Vol. 30, No. 6, pp. 74-77+96, (2011).

[29] C. H. Liu, *Study of finite element method for rotor-casing system vibration characteristic analysis*, MA thesis, Shenyang Aerospace University, Shenyang, Liaoning, (2016).

[30] R. R. Mutra, J. Srinivas and R. Rządkowski, "An optimal parameter identification approach in foil bearing supported high-speed turbocharger rotor system", *Arch. Appl. Mech.*, Vol. 91, No. 4, pp. 1557–1575, (2021).

[31] H. F. Wang, G. Chen, Z. K. Liao, Z. Zhang and F. Y. Shao, "Modeling for

[32] whole missile turbofan engine vibration with support looseness fault and characteristics of casing response", *J. Aerosp. Power*, Vol. 30, No. 3, pp. 627-638, (2015).

[32] R. R. Mutra and J. Srinivas, "Dynamic analysis of a turbocharger rotor-bearing system in transient operating regimes", *J. Inst. Eng. India Ser. C*, Vol. 101, No. 5, pp. 771–783, (2020).

[33] R. R. Mutra and J. Srinivas, "Parametric design of turbocharger rotor system under exhaust emission loads via surrogate model", *J Braz. Soc. Mech. Sci. Eng.*, Vol. 43, No. 3, pp. 117, (2021).

[34] J. Zhang, D. Y. Zhang, Y. F. Wang, Y. H. Ma and J. Hong, "Coupling vibration characteristics analysis of shared support-rotors system", *J. Beijing Univ. Aeronaut. Astronaut.*, Vol. 45, No. 9, pp. 1902-1910, (2019).

How to cite this paper:

Zhinong Li, Fang Qiao, Yunlong Li, Shiyao Chen, Shijian Zhou and Fei Wang, " Vibration characteristics of rotor systems with disk-shaft clearance,", *J. Comput. Appl. Res. Mech. Eng.,* Vol. 13, No. 2, pp. 123-136, (2024).

DOI: 10.22061/JCARME.2023.9410.2262

URL: https://jcarme.sru.ac.ir/?_action=showPDF&article=1950